

Dynamic metabolic profiling of urine biomarkers in rats with alcohol-induced liver damage following treatment with Zhi-Zi-Da-Huang decoction

LI AN¹, QIAOLING LANG¹, WENBIN SHEN², QINGSHUI SHI³ and FANG FENG^{1,4}

¹Department of Pharmaceutical Analysis; ²Center for Instrumental Analysis, China Pharmaceutical University, Nanjing, Jiangsu 210009; ³Jiangsu Institute for Food and Drug Control, Nanjing, Jiangsu 210008;

⁴Key Laboratory of Drug Quality Control and Pharmacovigilance, China Pharmaceutical University, Ministry of Education, Nanjing, Jiangsu 210009, P.R. China

Received July 21, 2015; Accepted May 26, 2016

DOI: 10.3892/mmr.2016.5494

Abstract. Alcoholic liver disease (ALD) is a leading cause of liver-associated morbidity and mortality. Zhi-Zi-Da-Huang decoction (ZZDHD), a traditional Chinese medicine formula, has been frequently used to treat or alleviate the symptoms of the various stages of ALD. To identify metabolic changes and the ZZDHD mechanism of action on ALD, potential urine biomarkers involved in the effects of ZZDHD were identified. Additionally, dynamic metabolomic profiles were systematically analyzed using nuclear magnetic resonance (NMR) spectroscopy in conjunction with statistical analysis. Alcohol administration to experimental rats disrupted multiple metabolic pathways, including methionine, gut bacterial, energy and amino acid metabolism. However, ZZDHD relieved certain effects of alcohol on the metabolism and regulated changes in potential characteristic biomarkers, including dimethylglycine, hippurate, lactate and creatine. The present study investigated time-dependent metabolomic changes in the development of alcohol-induced liver injury, including the effect of ZZDHD intervention. These findings elucidated important information regarding the metabolic responses to the protective effects of ZZDHD. ¹H NMR-based metabolomics method a reliable and useful tool for determining the metabolic progression of alcohol-induced liver injury and elucidating the underlying mechanisms of the effect of traditional Chinese medicine formulas. This study also demonstrated that NMR-based metabolomics approach is a powerful tool for understanding the molecular basis of pathogenesis and drug intervention processes.

Introduction

Alcoholic liver disease (ALD) is a complex disease with multifaceted metabolic abnormalities and has become a major life-threatening disease (1). The developmental progression of ALD ranges from fatty liver to hepatic inflammation, necrosis, progressive fibrosis and hepatocellular carcinoma, and the advanced-stage disease is difficult to treat successfully (2-4).

The underlying mechanisms of disease progression remain to be fully elucidated, which hinders the development of treatment therapies for ALD. Thus, there is remains no Food and Drug Administration-approved or widely accepted therapeutic agent for any of the stages of ALD. Traditional Chinese medicine (TCM) formulas have multiple targets, few toxic side effects and exert holistic therapeutic effects. TCM agents have been used for centuries to treat alcohol liver injury, with efficacy validated in a series of clinical experiments (5). Zhi-Zi-Da-Huang Decoction (ZZDHD), a classic TCM formula, which was first described in Jin-Kui-Yao-Lue, the classic clinical book of TCM (6). ZZDHD is a combination of four crude herbs, *Gardenia jasminoides* Ellis (Zhi-Zi), *Rheum officinale* Baill. (Da-Huang), *Citrus aurantium* L. (Zhi-Shi) and Semen Sojae Preparatum (Dan-Dou-Chi). ZZDHD has been commonly used to treat or alleviate the symptoms of alcoholic jaundice and ALD (6-8). However, the potential mechanisms that mediate the effects have not been fully elucidated.

Metabolomics, a powerful tool of systems biology, is defined as “quantitative measurement of time-related multiparametric metabolic response of living systems to pathophysiological stimuli or genetic modification” (9). It has been widely used for the assessment of disease models, early diagnosis and research on the mechanisms of therapeutic agents (9-14). Nuclear magnetic resonance (NMR)-based metabolomics, which is a highly sensitive, specific and useful tool to provide a rapid, non-destructive and relatively simple sample preparation (1,15-17), has been used for disease diagnosis, the identification of metabolic pathways associated with disease or drug treatment, and to elucidate biomarkers from biofluids (18-20). NMR-based metabolomics may also provide

Correspondence to: Professor Fang Feng, Department of Pharmaceutical Analysis, China Pharmaceutical University, 24 Tongjia Lane, Nanjing, Jiangsu 210009, P.R. China
E-mail: feng1fang1@126.com

Key words: Zhi-Zi-Da-Huang decoction, alcohol-induced liver injury, dynamic metabolic profiling, potential mechanisms

molecular insights into pathophysiology and therapeutic effects by tracking the dynamic changes of identified potential endogenous biomarkers, which makes it a useful method for the evaluation of the holistic and systematic effects of the TCM formula on ALD.

The present study used an NMR-based metabolomic approach to identify potential characteristic urinary biomarkers in rats with alcohol-induced liver damage following administration of ZZDHD, and subsequently determined the dynamic profiling of potential characteristic biomarkers identified in the alcohol or ZZDHD group rats compared with the control group rats in order to investigate specific changes to endogenous metabolites and the underlying mechanisms.

Materials and methods

Chemicals and reagents. Analytical grade sodium chloride, methanol, ethanol, acetic acid, $K_2HPO_4 \cdot 3H_2O$ and $NaH_2PO_4 \cdot 2H_2O$ were purchased from Nanjing Chemical Reagent Co., Ltd. (Nanjing, China). NaN_3 was obtained from Sinopharm Chemical Reagent Co., Ltd. (Shanghai, China). D_2O (99.9% D) and trimethylsilyl propionate (TSP) were obtained from Sigma-Aldrich (St. Louis, MO, USA). Phosphate buffer (K_2HPO_4/NaH_2PO_4 , 1.5 M, pH 7.4) prepared in D_2O containing 0.1% (w/v) TSP and 0.1% NaN_3 (w/v) was used for NMR sample preparation.

Preparation of the ZZDHD extract. All crude herbs were authenticated by Prof. Ping Li (Department of Medicinal Plants, China Pharmaceutical University, Nanjing, China). A mixture of 9 g *Gardenia jasminoides* Ellis, 3 g *Rheum officinale* Baill., 12 g *Citrus aurantium* L. and 24 g Semen Sojae Preparatum were extracted in 480 ml of distilled water and boiled for 30 min. The mixture was strained through a five-layer bandage. This procedure was repeated twice and the filtrate was freeze-dried for experimental usage. High-performance liquid chromatography analysis of freeze-dried ZZDHD powder is presented in Fig. 1.

Animal handling and sample collection. A total of 24 clean-grade, male Sprague-Dawley rats (age, 6 weeks; weight, 200 ± 20 g) were obtained from the Animal Multiplication Centre of Qinglong Mountain (Nanjing, China). All animal experiments were implemented strictly in accordance with the guidance for Experimental Animal Welfare of the National Guidelines at the Centre for SPF-grade Animal Experiments at the Jiangsu Institute for Food and Drug Control (Nanjing, China). The animals were housed in an animal facility with the following parameters: Temperature, $25 \pm 2^\circ C$; humidity, $60 \pm 5\%$ and artificial 12-h light/dark cycle. The animals were acclimatized for 7 days prior to experiments with access to the certified standard chow and water. Subsequently, the rats were randomly divided into three groups ($n=8$), the control group (CG), the alcohol group (AG) and the ZZDHD group (ZG). Water was orally administered to the control rats between 5:00 pm and 6:00 pm from day 1-8. The AG rats received water orally between 5:00 pm and 6:00 pm from day 1-2 and then 50% alcohol at a dose of 5 g/kg/day from day 3-8. The ZG rats were orally treated with freeze-dried ZZDHD powder at a dose of 12 g/kg/day between 3:00 pm and 4:00 pm from day 1-8.

Simultaneously, the ZG rats were also orally administered with 50% alcohol at a dose of 5 g/kg/day between 5:00 pm and 6:00 pm from day 3-8. All overnight urine samples for each rat were collected (from 8:00 pm to 8:00 am) manually to prevent contamination on days 0, 3, 4, 5, 6, 7 and 8. Urine collection tubes were stored at low temperatures ($0-4^\circ C$) using a cooling bath and NaN_3 solution (0.1% w/v) was added to inhibit bacterial growth. The urine samples were stored at $-80^\circ C$ prior to 1H NMR analysis. At 8:00 pm on day 8, all animals were fasted and then euthanized after 12 h using 4% isoflurane anesthesia (Shandong Keyuan Pharmaceutical Co., Ltd., Jinan, China). The liver and serum samples from all groups were collected immediately on day 9 (8:00 am). The experimental procedures were approved by the Animal Care and Ethics Committee at the Jiangsu Institute for Food and Drug Control. All surgeries were performed under isoflurane anesthesia and all efforts were made to ameliorate the suffering of the animals.

Biochemical analysis and histology assay. Alanine aminotransferase (ALT) and aspartate aminotransferase (AST) activities, liver superoxide dismutase (SOD) activity, and glutathione (GSH) and malondialdehyde (MDA) concentration in the liver homogenate were analyzed with commercial kits according to the manufacturer's protocol in the Experiment Centre at the Jiangsu Institute for Food and Drug Control (Jiangsu, China). The assay kits for AST (cat. no. 20121007), ALT (cat. no. 20121010), SOD (cat. no. 20121209), GSH (cat. no. 20121208) and MDA (cat. no. 20121211) were purchased from the Nanjing Jiancheng Bioengineering Institute (Nanjing, China). The biochemical parameters were calculated and expressed as the mean \pm standard deviation and $P < 0.05$ was considered to indicate a statistically significant difference. For hematoxylin and eosin staining, a portion of the same liver lobe in each rat was immediately fixed via immersion in 10% neutral-buffered formalin, embedded in paraffin and sectioned into slices of 4-5 μm . For the remaining liver tissue, Oil red O staining was performed on 10-15 μm frozen liver sections.

NMR spectroscopy and statistical analysis. Frozen urine samples were thawed at room temperature. A total of 500 μl urine was analyzed following the addition of 50 μl D_2O solution, this addition provided a lock signal containing 5 mM TSP as a reference for the chemical shift. The mixture was centrifuged at $16,099 \times g$ for 10 min at $4^\circ C$. These solutions were then transferred to 5 mm NMR tubes. For each sample, a 1H NMR spectrum was acquired on a Bruker AV 500 MHz spectrometer at 300 K and recorded using a standard NOESYPR1D pulse sequence (recycle delay- 90° - t_1 - 90° - t_m - 90° -acquisition). The 1H NMR spectra were determined using 160 scans spectra and a Fourier transform was used, following an exponential line-broadening function of 0.25 Hz. All urinary spectra were then manually phased, baseline corrected and referenced to TSP (CH_3 , δ 0.0) using TOPSPIN software (version 2.1, Bruker Biospin GmbH, Rheinstetten, Germany).

All 1H NMR spectra were processed using the AMIX software package (Bruker Biospin GmbH). Regions from 0.5-4.5 and 5.98-9.5 ppm were included in the integration, as regions ≤ 0.5 and ≥ 9.5 ppm contained only noise, and the spectral region 4.50-5.98 ppm contained the suppression of water resonances and cross-relaxation effects. To account

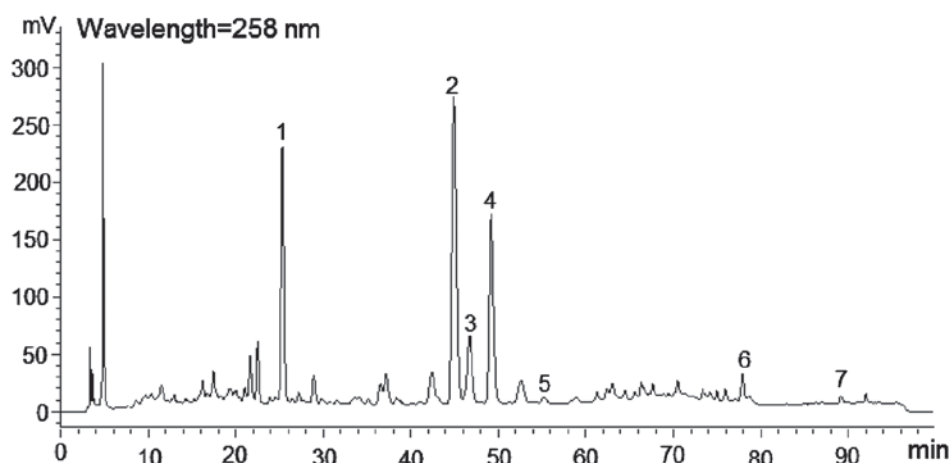


Figure 1. High-performance liquid chromatography-UV fingerprint of Zhi-Zi-Da-Huang decoction at (258 nm). Mobile phase: (a) 0.1% acetic acid; (b) methanol; non-linear gradient elution. Peaks: (1) geniposide, (2) naringin, (3) hesperidin, (4) neohesperidin, (5) daidzein, (6) rhein, (7) emodin.

for the presence of ethanol and ethyl glucuronide (EtG) in the samples from the AG, the spectra were integrated into bins with a width of 0.04 ppm, following the removal of the bins that contained the ethanol and EtG peaks (21) and then normalized via probabilistic quotient normalization. A multivariate data analysis was performed using the software package SIMCA-P (version 13.0, Umetrics, Malmö, Sweden). Orthogonal projection to latent structure discriminant analysis (OPLS-DA), a supervised multivariate data analysis tool, was used with 7-fold cross-validation and the pareto-scaled data as the X-matrix and the class information as the Y-matrix in order to identify metabolites with significant intergroup differences. The fit of the models were evaluated using R^2X and Q^2 , which respectively represent the explained variations and predictability of the models. Values of these parameters near 1.0 indicated an effective and stable model, with predictive reliability. All models were additionally tested using the cross-validated analysis of variance approach. $P < 0.05$ was considered to indicate a statistically significant difference. A univariate analysis was also applied to verify statistically significant metabolites using parametric (Student's *t*-test) or nonparametric (Mann-Whitney test) tests for potential characteristic biomarkers.

To obtain the dynamic changes of potential characteristic biomarkers following ZZDHD intervention, the ratios of the metabolites were calculated for the corresponding time points in the forms of $[F_A - F_C]/F_C$ and $[F_Z - F_C]/F_C$, where F_A , F_C and F_Z stood for the average metabolite concentrations of the corresponding metabolites following probabilistic quotient normalization in the AG, CG and ZG, and these results were expressed as a line graph.

Results

Effects of ZZDHD on biochemical indicators and histopathological examination of rats with alcohol-induced liver damage. To determine the hepatoprotective effects of ZZDHD, the levels of serum AST and ALT and liver SOD, GSH and MDA were detected. The biochemical analysis indicated that the levels of AST, ALT, SOD, GSH and MDA were significantly changed in the AG compared with the CG

and ZG ($P < 0.05$; Table I). AG rats had significantly higher levels of AST and ALT in the serum compared with the CG ($P < 0.05$). AST and ALT activity in the serum are typically low, however, the levels of ALT and AST increase in the event of liver injury. The levels of SOD and GSH were significantly decreased ($P < 0.05$), and MDA levels were significantly increased, in the AG compared with the CG ($P < 0.05$). However, the biochemical indicators, including serum AST, ALT, liver SOD, GSH and MDA, were markedly improved in the ZG compared with the AG ($P < 0.05$; Table I). Thus, when combined with alcohol treatment, the ZZDHD alleviated alcohol-induced liver damage.

In order to investigate the protective effects of ZZDHD on hepatic tissue damage, histological analysis was conducted on rat liver tissues (Fig. 2). The CG rats exhibited normal liver tissue and no pathological changes were observed (Fig. 2A), with a similar phenomenon observed following Oil red O staining (Fig. 2B). However, the AG rats exhibited fat particles of varying sizes (Fig. 2C and D), thus presenting a degree of hepatic injury. Histological examination of the ZG did not indicate any observable fat particles (Fig. 2E and F); thus, ZZDHD may ameliorate the hepatic steatosis of rats with alcohol-induced liver damage.

Identification of potential characteristic biomarkers in rat urine. The typical 1H NMR spectra of rat urine are presented in Fig. 3 for the CG, AG and ZG, with major metabolites labeled. With respect to the identification of differential metabolites, the corresponding chemical shifts of the metabolites were previously described (22-25) and are publicly accessible in metabolomic databases, including Madison (www.mmcd.nmr.fam.wisc.edu), Kyoto Encyclopedia of Genes and Genomes (www.genome.jp/kegg/) and the Human Metabolome Database (www.hmdb.ca), and using Chenomx NMR Suite software (version 7.5, Chenomx, Inc., Edmonton, Canada). The detectable metabolites in these spectra included ethanol, EtG, acetate, taurine, glycine, lactate, creatinine, creatine, N-acetyl glycoproteins, dimethylamine (DMA), dimethylglycine (DMG), methylamine and tricarboxylic acid cycle intermediates (citrate, α -ketoglutarate and succinate), hippurate, trigonelline and formate. Compared with the CG,

Table I. Physiological and biochemical characteristics from the serum and liver of rats in control, alcohol and ZZZDHD groups.

Clinical chemistry data	Control group	Alcohol group	ZZDHD group
ALT (IU/l)	32.97±1.20 ^b	58.53±6.22	45.32±7.93 ^a
AST (IU/l)	46.89±15.64 ^a	106.16±27.96	85.01±17.73 ^a
SOD (μ/mgprot)	266.95±50.05 ^a	167.99±24.96	215.23±13.62 ^a
GSH (mg/mgprot)	28.65±3.58 ^a	19.11±2.20	24.19±2.89 ^a
MDA (nmol/mgprot)	1.14±0.36 ^a	2.43±0.60	1.41±0.55 ^a

Data are expressed as the mean ± standard deviation. ^aP<0.05 vs. alcohol group. ^bP<0.01 vs. alcohol group. ZZZDHD, Zhi-Zi-Da-Huang decoction; ALT, alanine aminotransferase; AST, aspartate aminotransferase; SOD, superoxide dismutase; GSH, glutathione; MDA, malondialdehyde.

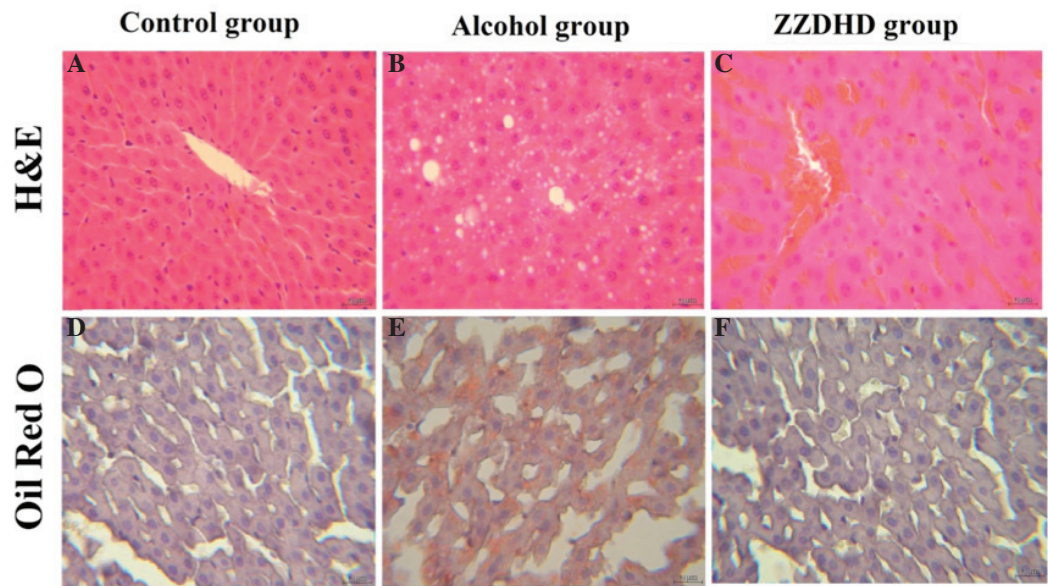


Figure 2. Representative liver sections from (A and B) control, (C and D) alcohol and (E and F) ZZZDHD rat groups. Sections were stained with (A, C and E) hematoxylin and eosin for evaluation of fatty deposition, confirmed by (B, D and F) Oil Red O. ZZZDHD, Zhi-Zi-Da-Huang decoction; H&E, hematoxylin and eosin.

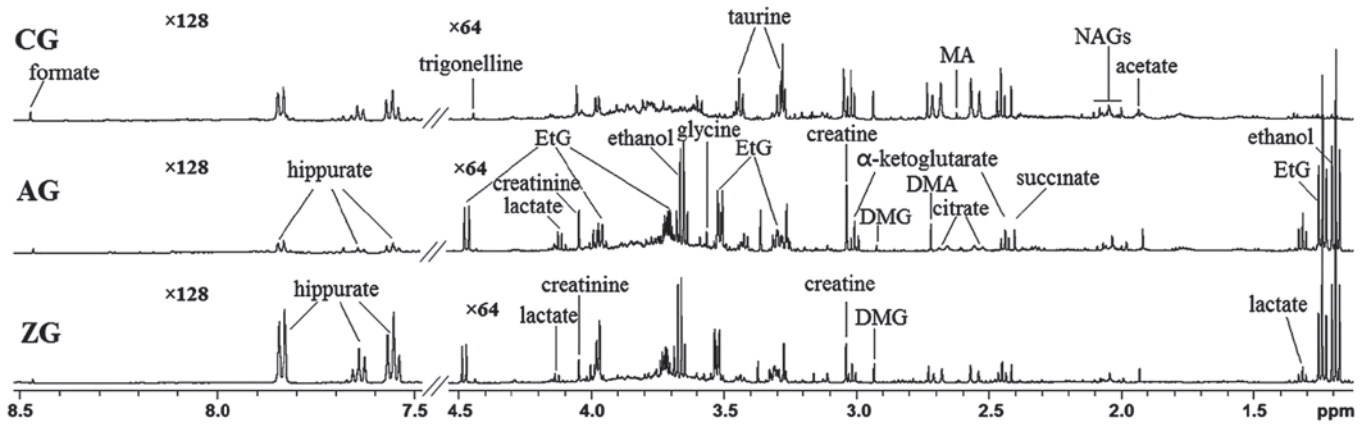


Figure 3. Nuclear magnetic resonance 500 MHz ¹H spectra (δ8.5~7.5, δ4.5~1.1 ppm) of rat urine obtained from CG, AG and ZG. CG, control group; AG, alcohol group; ZG, Zhi-Zi-Da-Huang decoction group; EtG, ethyl glucuronide; DMG, dimethylglycine; DMA, dimethylamine; MA, methylamine; NAGs, N-acetyl glycoproteins.

the primary differences in the AG were the appearance of ethanol and EtG, an increase in creatine, lactate and glycine, and a decrease in hippurate, DMG, DMA and tricarboxylic acid cycle intermediates. In the ZG compared with the AG,

hippurate and DMG levels were increased, whereas creatinine and lactate levels were decreased. Additionally, hippurate levels in the ZG were significantly increased compared with the AG, and were even higher compared with the CG.

Table II. Changes in rat urine metabolites from AG vs. CG and ZG vs. AG on day 8.

No.	Metabolite	Chemical shift (ppm)	AG vs. CG		ZG vs. AG	
			VIP ^a	P ^b	VIP ^a	P ^b
1	Hippurate	7.56(t), 7.64(t), 7.84(d)	3.34	0.000	2.89	0.001
2	Lactate	1.32(d), 4.12(q)	5.64	0.002	2.91	0.005
3	Glycine	3.56(s)	2.86	0.006	-	n.s.
4	Creatine	3.04(s)	6.38	0.009	3.25	0.013
5	DMA	2.72(s)	2.10	0.000	-	n.s.
6	DMG	2.92(s)	1.87	0.000	1.03	0.003
7	α -Ketoglutarate	2.44(t), 3.00(t)	1.48	n.s.	1.07	n.s.
8	Citrate	2.56(d), 2.68(d)	2.61	0.002	-	0.003
9	Succinate	2.40(s)	1.03	0.021	-	n.s.

^aObtained from orthogonal projection to latent structure discriminant analysis with a threshold 1.0, indicates the VIP value is >1. ^bP-values were calculated by Student's t-test or Mann-Whitney test. s, singlet; d, doublet; t, triplet; q, quartet; n.s., no significant difference; AG, alcohol group; CG, control group; ZG, ZZDHD group; DMA, dimethylamine; DMG, dimethylglycine; VIP, variable importance in the projection.

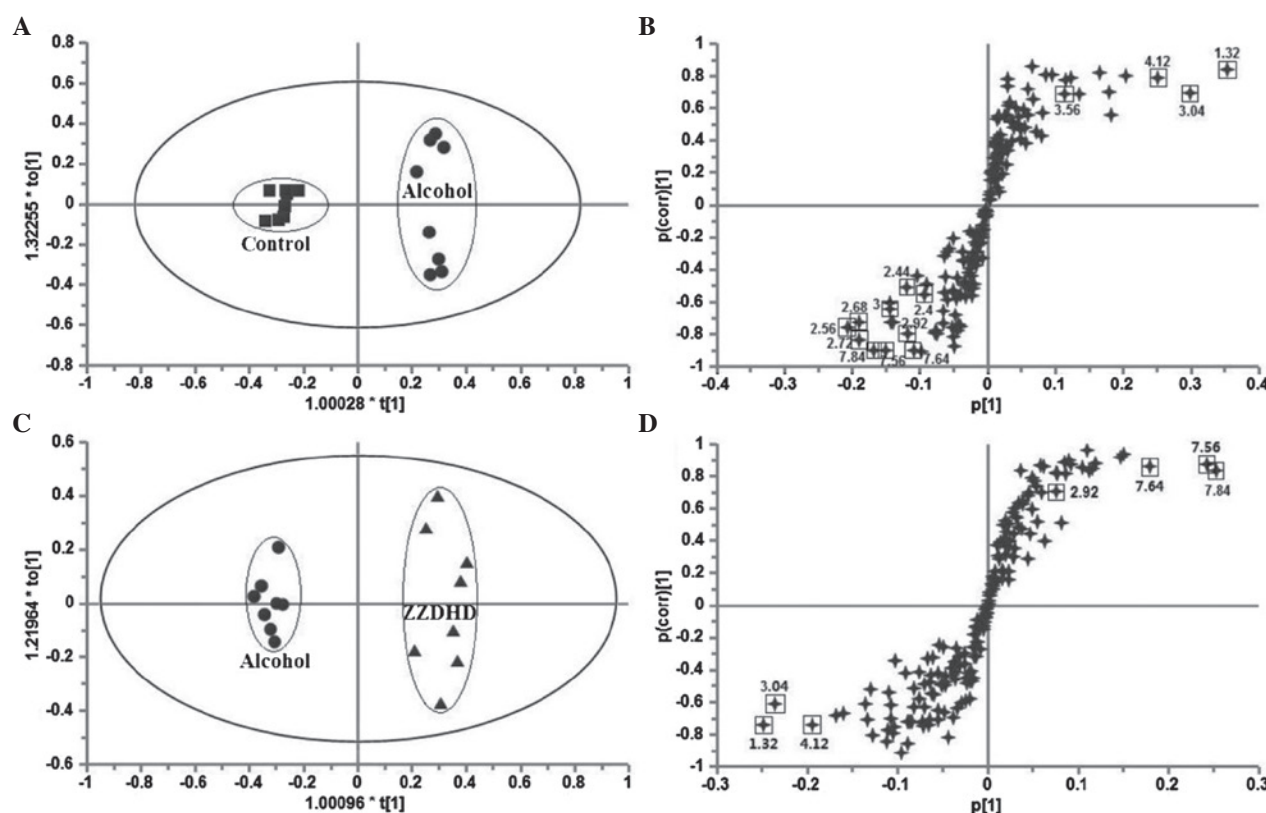


Figure 4. Multivariate statistical analysis of ¹H nuclear magnetic resonance spectra of rat urine samples on day 8. Orthogonal projection to latent structure discriminant analysis scores plots derived from (A) AG vs. CG with (B) the corresponding S-plot, and (C) ZG vs. AG with (D) the corresponding S-plot. The marked triangles in (B) and (D) may be regarded as potential differential metabolites. ZZDHD, Zhi-Zi-Da-Huang decoction; CG, control group; AG, alcohol group; ZG, ZZDHD group.

Analysis of urine metabolomics data. To obtain further details regarding metabolic changes and to identify potential characteristic biomarkers, which represent the effect of ZZDHD on alcohol-induced liver damage, multivariate and univariate analyses were conducted on the NMR data on day 8 (Table II). OPLS-DA was performed to determine if there were significant differences in the metabolites of the different treatment

groups. A clear separation between the AG and CG (Fig. 4A) was demonstrated and significant metabolomic differences with good model fit ($R^2X=0.845$, $Q^2=0.907$, $P=3.54 \times 10^{-4}$) were observed. The corresponding S-plot (Fig. 4B) distinguished nine metabolites. Lactate, creatine and glycine were increased in the AG compared with CG, and were located in the upper-right quadrant. The decreased metabolites, including

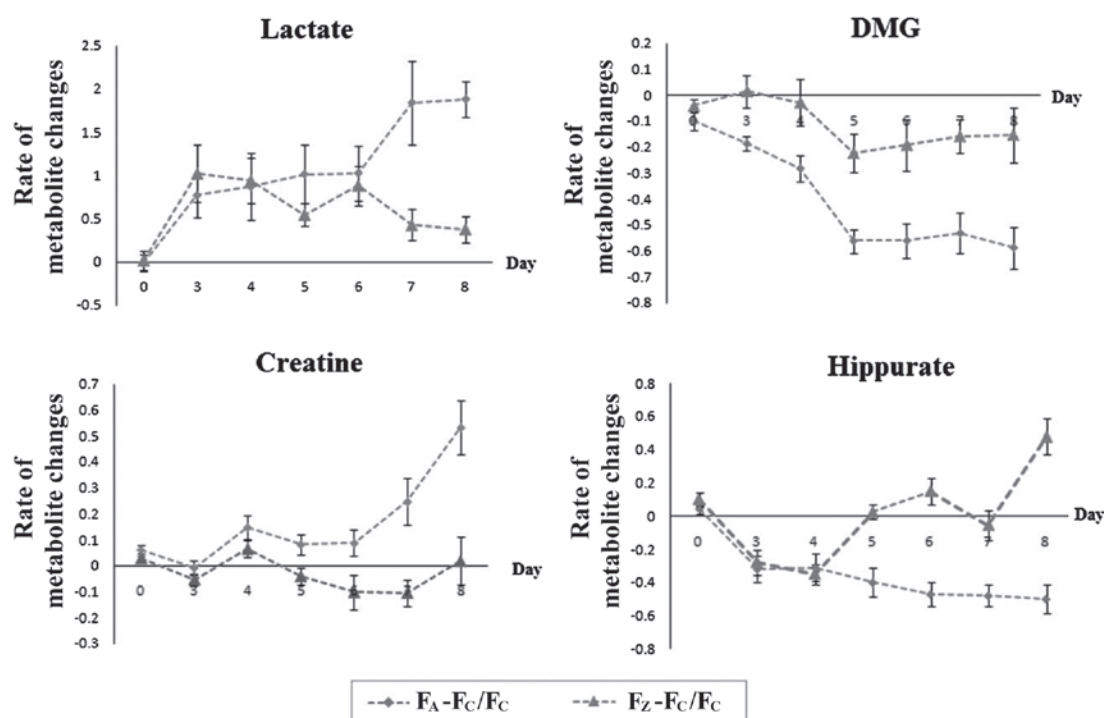


Figure 5. Ratios of dynamic changes for the potential urine characteristic biomarkers with ZZDHD intervention for alcohol-treated rats or ZZDHD rats relative to control rats. ZZDHD, Zhi-Zi-Da-Huang decoction; DMG, dimethylglycine; F_A , alcohol group concentration; F_C , control group concentration; F_Z , ZZDHD group concentration.

hippurate, TCA cycle intermediates, DMG and DMA, were located in the lower-left quadrant. The score plot of OPLS-DA for AG and ZG (Fig. 4C) indicated a clear separation between the two groups ($R^2X=0.523$, $Q^2=0.936$, $P=1.68 \times 10^{-6}$) and four metabolites exhibited changes in the S-plot (Fig. 4D), including hippurate and DMG increased in the ZG, while creatine and lactate levels were decreased.

The altered urine metabolites described above from the AG compared with CG and ZG were validated via variable importance in the projection (VIP) using a $VIP \geq 1$. The P-values for the detected metabolites in the different groups were calculated using Student's t-test or Mann-Whitney test. The results demonstrated that the levels of metabolites, including lactate, creatine, hippurate and DMG, were significantly altered following ZZDHD intervention. Thus, these four metabolites may be potential characteristic biomarkers of the intervention effects of ZZDHD on alcohol-induced liver damage. The present study demonstrated that alcohol administration disrupted energy, amino acid, methionine and gut bacterial metabolism. The results indicated that ZZDHD partially regulated the altered metabolic changes induced by alcohol to promote a return to basal levels, which was also validated by the assessment of biochemical indicators and histopathology.

Dynamic metabolic profiling of potential characteristic biomarkers. The ratios of the four potential characteristic biomarkers, including lactate, hippurate, DMG and creatine were calculated as AG or ZG relative to CG (Fig. 5), in order to investigate the changes and dynamic effects in the occurrence, development and ZZDHD intervention of early-stage alcoholic liver injury. All four metabolites exhibited time-dependent

changes. The ratio of lactate in the AG compared with the CG varied between 0.8 and 1 from day 3-6. Lactate exhibited a nearly 2-fold increase, with a maximum level observed on day 5 following ethanol administration. Lactate in the ZG, relative to the CG, ranged between 0.6 and 1 from day 3-6; however, this ratio was approximately 5-fold lower compared with the AG after day 7 and 8. The ratio of DMG in the AG (relative to CG) decreased between 0.22 and 0.31 on day 3 and 4, and it was 0.6 from day 5-8, which suggested that DMG was reduced compared with the controls during ethanol treatment from day 5-8. The DMG level in the ZG was maintained below 0.22 compared with the CG during ethanol administration. Creatine increased to 0.27 on day 7 and to 0.52 on day 8 in the AG compared with the CG. The creatine in the ZG remained constant compared with the CG rats. The hippurate in the AG was decreased to ~ 0.3 on day 3 and 4, and was lower than 0.4 from day 5-8 in the corresponding period. The hippurate level in the ZG exhibited similar changes to the AG compared with the CG rats on day 3 and 4, that remained unchanged compared with CG rats from day 5 to day 7 and increased to >0.4 on day 8. This indicated that ZZDHD altered the gut bacteria to restore the normal metabolism of hippuric acid, with increased production of hippurate due to the polyphenols of ZZDHD. Metabolite changes were observed in the AG and the ZG compared with the CG for lactate, DMG, creatine, and hippurate.

Discussion

The present study investigated the hepatoprotective effects of ZZDHD on alcohol-induced liver damage. Additionally, the current study investigated the dynamic metabolic variations

in potential characteristic biomarkers that changed following ZZDHD intervention and the underlying mechanisms involved.

Alcohol metabolism leads to redox state changes in the nicotinamide adenine dinucleotide (NAD⁺)/reduced nicotinamide adenine dinucleotide (NADH) ratio, including excessive generation of reactive oxygen species and oxidative stress (26-28). This results in mitochondrial dysfunction, which further disturbs normal metabolism. Lactate, a metabolic product of glycolysis, maintains normal energy metabolism. Pyruvate is converted to lactate by lactic dehydrogenase during hypoxia. The NADH/NAD⁺ ratio also affects the production of lactic acid. As a consequence of ethanol metabolism, the NADH/NAD⁺ redox ratio increases as ethanol is oxidized to acetaldehyde, and acetic acid and the vitamin cofactor NAD⁺ of these two processes is reduced to NADH (29-31). Increased NADH accelerates the transformation of pyruvate to lactate. Additionally, hypoxia has been demonstrated in ethanol metabolism (32). In the current study, the lactate levels in the AG were significantly increased from day 7, indicating that energy metabolism may be different from normal. The lactate levels in the ZG were lower compared with the AG. However, they were similar to the CG on day 8, indicating that ZZDHD reduced the level of lactate and restored the energy metabolism to a normal level. ZZDHD may relieve the abnormal effects of liver injury by regulating energy metabolism.

Alcohol and its metabolites have been previously demonstrated to affect the methionine metabolic pathway (33-35) by increasing the activity of betaine-homocysteine methyltransferase (BHMT) and decreasing the activity of cystathionine β -synthase (C β S) (36). Betaine is demethylated by BHMT to produce DMG, and homocysteine is synchronously transformed to methionine (37). Thus, DMG production may increase due to improved BHMT activity; however, a significant reduction in DMG was observed in the AG from day 5-8. This may be due to DMG not being excreted directly into the urine, or it may have been metabolized to glycine and then to creatine (38). The creatine levels in the AG compared with the CG were significantly increased to 0.52 following 6 days of exposure to alcohol, whereas the creatine levels in the ZG did not exhibit any observable change compared with the CG. ZZDHD significantly improved the levels of DMG and creatine. This indicated that ZZDHD treatment may ameliorate disrupted methionine metabolism caused by alcohol, as demonstrated by its abilities to restore the levels of DMG and creatine to near normal levels.

Benzoic acid, the precursor of hippurate, is produced by gut microflora (39). Decreased DMA and hippurate levels are indicators of a damaged intestinal environment. Additionally, hippurate, which is the glycine conjugate of benzoic acid, is formed in the mitochondria of liver cells, in which the conversion from benzoic acid to benzoyl-CoA requires adenosine triphosphate (ATP). Therefore, reduced ATP due to mitochondrial dysfunction also affects the generation of hippurate. A previous study reported that glycine availability is an important factor in determining hippurate production (40). In the present study, increased glycine content and decreased hippurate content in the AG suggested that the change observed in hippurate levels may also be attributed

to mitochondrial dysfunction. The dynamic changes of hippurate suggested that ethanol administration disrupted the intestinal flora and ZZDHD alleviated the extent of this disturbance, which may contribute to its protective mechanism.

The present study used a ¹H NMR-based metabolomics approach to determine the metabolic profiles of rats in different groups and identify potential characteristic biomarkers of the hepatoprotective effects of the ZZDHD on alcohol-induced liver injury. Furthermore, time-course urinary metabolic responses of rats to ZZDHD intervention indicated that DMG, hippurate, lactate and creatine are important biomarkers for the specific processes affected by ZZDHD. It was demonstrated that ZZDHD regulated the abnormal metabolic state by interfering with different metabolic pathways, including energy, amino acid, methionine and gut bacterial metabolism. The present study also demonstrated that the ¹H NMR-based metabolomics method is a useful tool for determining the potential molecular mechanisms of the TCM formulas on hepatic injury and investigating their mode of action by identifying potential characteristic biomarkers.

Acknowledgements

The present study was supported by National Natural Science Foundation of China (grant no. 81274063) and a Project Funded by the Priority Academic Program Development of Jiangsu Higher Education Institutions.

References

1. Rehm J, Samokhvalov AV and Shield KD: Global burden of alcoholic liver diseases. *J Hepatol* 59: 160-168, 2013.
2. Gao B and Bataller R: Alcoholic liver disease: Pathogenesis and new therapeutic targets. *Gastroenterology* 141: 1572-1585, 2011.
3. Li YM, Fan JG, Wang BY, Lu LG, Shi JP, Niu JQ and Shen W: Chinese Association for the Study of Liver Disease: Guidelines for the diagnosis and management of alcoholic liver disease: Update 2010: (Published in Chinese on Chinese Journal of Hepatology 2010; 18: 167-170). *J Dig Dis* 12: 45-50, 2011.
4. Ramaiah S, Rivera C and Arteel G: Early-phase alcoholic liver disease: An update on animal models, pathology, and pathogenesis. *Int J Toxicol* 23: 217-231, 2004.
5. Tan H Y, Serban S M, Wang N, Hong M, Li S, Li L, Cheung F, Wen X Y, Feng Y B: Preclinical Models for Investigation of Herbal Medicines in Liver Diseases: Update and Perspective. *Evid Based Complement Alternat Med* 2016: 4750163, 2016.
6. Chen JC: Hypothesis and clinical study of modular formulation. *Journal of Chinese Medicine* 12: 69-80, 2001.
7. An L and Feng F: Network pharmacology-based antioxidant effect study of Zhi-Zi-Da-Huang decoction for alcoholic liver disease. *Evid Based Complement Alternat Med* 2015: 492470, 2015.
8. Wang H, Feng F, Zhuang BY and Sun Y: Evaluation of hepatoprotective effect of Zhi-Zi-Da-Huang decoction and its two fractions against acute alcohol-induced liver injury in rats. *J Ethnopharmacol* 126: 273-279, 2009.
9. Nicholson JK, Lindon JC and Holmes E: 'Metabonomics': Understanding the metabolic responses of living systems to pathophysiological stimuli via multivariate statistical analysis of biological NMR spectroscopic data. *Xenobiotica* 29: 1181-1189, 1999.
10. Ghauri FY, Nicholson JK, Sweatman BC, Wood J, Beddell CR, Lindon JC and Cairns NJ: NMR spectroscopy of human post mortem cerebrospinal fluid: Distinction of Alzheimer's disease from control using pattern recognition and statistics. *NMR Biomed* 6: 163-167, 1993.

11. Brindle JT, Antti H, Holmes E, Tranter G, Nicholson JK, Bethell HW, Clarke S, Schofield PM, McKilligan E, Mosedale DE and Grainger DJ: Rapid and noninvasive diagnosis of the presence and severity of coronary heart disease using ¹H-NMR-based metabolomics. *Nat Med* 8: 1439-1444, 2002.
12. Yang J, Xu G, Kong H, Zheng Y, Pang T and Yang Q: Artificial neural network classification based on high-performance liquid chromatography of urinary and serum nucleosides for the clinical diagnosis of cancer. *J Chromatogr B Analyt Technol Biomed Life Sci* 780: 27-33, 2002.
13. Li J, Yang L, Li Y, Tian Y, Li S, Jiang S, Wang Y and Li X: Metabolomics study on model rats of chronic obstructive pulmonary disease treated with Bu-Fei Jian-Pi. *Mol Med Rep* 11: 1324-1333, 2015.
14. Huang M, Liang Q, Li P, Xia J, Wang Y, Hu P, Jiang Z, He Y, Pang L, Han L, *et al*: Biomarkers for early diagnosis of type 2 diabetic nephropathy: A study based on an integrated biomarker system. *Mol Biosyst* 9: 2134-2141, 2013.
15. Griffin JL: Metabonomics: NMR spectroscopy and pattern recognition analysis of body fluids and tissues for characterisation of xenobiotic toxicity and disease diagnosis. *Curr Opin Chem Biol* 7: 648-654, 2003.
16. Lin WN, Lu HY, Lee MS, Yang SY, Chen HJ, Chang YS and Chang WT: Evaluation of the cultivation age of dried ginseng radix and its commercial products by using (1)H-NMR fingerprint analysis. *Am J Chin Med* 38: 205-218, 2010.
17. Saric J, Wang Y, Li J, Coen M, Utzinger J, Marchesi JR, Keiser J, Veselkov K, Lindon JC, Nicholson JK and Holmes E: Species variation in the fecal metabolome gives insight into differential gastrointestinal function. *J Proteome Res* 7: 352-360, 2008.
18. Diao C, Zhao L, Guan M, Zheng Y, Chen M, Yang Y, Lin L, Chen W and Gao H: Systemic and characteristic metabolites in the serum of streptozotocin-induced diabetic rats at different stages as revealed by a (1)H-NMR based metabolomic approach. *Mol Biosyst* 10: 686-693, 2014.
19. Shi X, Wei X, Koo I, Schmidt RH, Yin X, Kim SH, Vaughn A, McClain CJ, Arteel GE, Zhang X and Watson WH: Metabolomic analysis of the effects of chronic arsenic exposure in a mouse model of diet-induced Fatty liver disease. *J Proteome Res* 13: 547-554, 2014.
20. Liu P, Duan J, Wang P, Qian D, Guo J, Shang E, Su S, Tang Y and Tang Z: Biomarkers of primary dysmenorrhea and herbal formula intervention: An exploratory metabolomics study of blood plasma and urine. *Mol Biosyst* 9: 77-87, 2013.
21. Nicholas PC, Kim D, Crews FT and Macdonald JM: Proton nuclear magnetic resonance spectroscopic determination of ethanol-induced formation of ethyl glucuronide in liver. *Anal Biochem* 358: 185-191, 2006.
22. Liu Y, Huang R, Liu L, Peng J, Xiao B, Yang J, Miao Z and Huang H: Metabonomics study of urine from Sprague-Dawley rats exposed to Huang-yao-zi using (1)H NMR spectroscopy. *J Pharm Biomed Anal* 52: 136-141, 2010.
23. Bradford BU, O'Connell TM, Han J, Kosyk O, Shymonyak S, Ross PK, Winnike J, Kono H and Rusyn I: Metabolomic profiling of a modified alcohol liquid diet model for liver injury in the mouse uncovers new markers of disease. *Toxicol Appl Pharmacol* 232: 236-243, 2008.
24. Sun YJ, Wang HP, Liang YJ, Yang L, Li W and Wu YJ: An NMR-based metabolomic investigation of the subacute effects of melamine in rats. *J Proteome Res* 11: 2544-2550, 2012.
25. Xu W, Wu J, An Y, Xiao C, Hao F, Liu H, Wang Y and Tang H: Streptozotocin-induced dynamic metabolomic changes in rat biofluids. *J Proteome Res* 11: 3423-3435, 2012.
26. Riveros-Rosas H, Julian-Sanchez A, Pina E and Pinã E: Enzymology of ethanol and acetaldehyde metabolism in mammals. *Arch Med Res* 28: 453-471, 1997.
27. Cederbaum AI: Alcohol metabolism. *Clin Liver Dis* 16: 667-685, 2012.
28. Kennedy NP and Tipton KF: Ethanol metabolism and alcoholic liver disease. *Essays Biochem* 25: 137-195, 1990.
29. Zakhari S: Overview: How is alcohol metabolized by the body? *Alcohol Res Health* 29: 245-254, 2006.
30. Gordon ER: The effect of chronic consumption of ethanol on the redox state of the rat liver. *Can J Biochem* 50: 949-957, 1972.
31. Veech RL, Guynn R and Veloso D: The time-course of the effects of ethanol on the redox and phosphorylation states of rat liverm. *Biochem J* 127: 387-397, 1972.
32. Arteel GE, Iimuro Y, Yin M, Raleigh JA and Thurman RG: Chronic enteral ethanol treatment causes hypoxia in rat liver tissue in vivo. *Hepatology* 25: 920-926, 1997.
33. Ji C: Mechanisms of alcohol-induced endoplasmic reticulum stress and organ injuries. *Biochem Res Int* 2012: 216450, 2012.
34. Halsted CH and Medici V: Aberrant hepatic methionine metabolism and gene methylation in the pathogenesis and treatment of alcoholic steatohepatitis. *Int J Hepatol* 2012: 959746, 2012.
35. Kharbanda KK: Alcoholic liver disease and methionine metabolism. *Semin Liver Dis* 29: 155-165, 2009.
36. Tsukamoto H and Lu SC: Current concepts in the pathogenesis of alcoholic liver injury. *FASEB J* 15: 1335-1349, 2001.
37. McGregor DO, Dellow WJ, Lever M, George PM, Robson RA and Chambers ST: Dimethylglycine accumulates in uremia and predicts elevated plasma homocysteine concentrations. *Kidney Int* 59: 2267-2272, 2001.
38. Wei L, Liao P, Wu H, Li X, Pei F, Li W and Wu Y: Metabolic profiling studies on the toxicological effects of realgar in rats by (1)H NMR spectroscopy. *Toxicol Appl Pharmacol* 234: 314-325, 2009.
39. Keller W: Keller on the conversion of benzoic into hippuric acid. *Prov Med J Retrospect Med Sci* 4: 256-257, 1842.
40. Beliveau GP and Brusilow SW: Glycine availability limits maximum hippurate synthesis in growing rats. *J Nutr* 117: 36-41, 1987.